Thermochimica Acta, 176 (1991) 209–220
Elsevier Science Publishers B.V., Amsterdam

THE DETERMINATION OF THE MOST PROBABLE MECHANISM FUNCTION AND KINETIC PARAMETERS OF THE THERMAL DECOMPOSITION OF COMPLEXES OF RARE EARTH ISOTHIOCYANATES WITH GLYCINE BY NON-ISOTHERMAL DIFFERENTIAL SCANNING CALORIMETRY CURVE

SHU-RONG YANG, JIAN-HUA ZHANG and BEN-GAO JIANG *

Department of Chemistry, Shandong University (People's Republic of China)

ZHAO-HE YANG

Institute of Crystal Materials, Shandong University (People's Republic of China)

(Received 21 May 1990)

ABSTRACT

The kinetics of thermal decomposition of the complexes $RE(NCS)_3 \cdot 3Gly \cdot H_2O$ (RE = Ce, Pr or Nd; Gly = glycine) were studied under non-isothermal condition by DSC. Kinetic parameters were obtained from analysis of the DSC curves by integral and differential methods. The most probable mechanism function was suggested by comparison of the kinetic parameters. A mathematical expression for the kinetic compensation effect was also derived. Some valuable results have been obtained and are analysed with discussion.

INTRODUCTION

Glycine is one of the α-amino-acids, which are very important in biology and medicine. Great interest has been aroused in the study of the coordination chemistry of α-amino-acids with metals. Complexes of rare earth chlorides with glycine have been prepared [1,2], but the preparation and properties of complexes of rare earth isothiocyanates with glycine have not yet been studied.

In this paper, we prepared three complexes $RE(NCS)_3 \cdot 3Gly \cdot H_2O$ (RE = Ce, Pr or Nd; Gly = glycine). The IR spectra and X-ray diffraction of the complexes were studied. The kinetics of the thermal decomposition reaction of $RE(NCS)_3 \cdot 3Gly \cdot H_2O$ were studied under non-isothermal conditions by DSC. The most probable mechanism function and kinetic parameters (apparent activation energy E and pre-exponential constant A) of the thermal

* To whom correspondence should be addressed.

0040-6031/91/$03.50

decomposition reaction of $RE(NCS)_3 \cdot 3Gly \cdot H_2O$ were determined, and a mathematical expression for the kinetic compensation effect was also derived.

EXPERIMENTAL

Purity of reagents and preparation of the complexes

Glycine was purified by means of recrystallization. The purified glycine was kept in a desiccator containing $CaCl_2$ until its weight became constant.

The complexes $RE(NCS)_3 \cdot 7H_2O$ (RE = Ce, Pr or Nd) were prepared as previously described [3].

To prepare $RE(NCS)_3 \cdot 3Gly \cdot H_2O$, $RE(NCS)_3 \cdot 7H_2O$ and glycine (in molar ratio 1 : 3) were dissolved in distilled water. The clear solution was concentrated in a desiccator containing phosphorus pentoxide until crystals were obtained. The crystals were filtered off and dried over phosphorus pentoxide until their weight became constant. The resulting complex was $RE(NCS)_3 \cdot 3Gly \cdot H_2O$.

Component analysis of the complexes

The rare earth content in the complex was determined by EDTA titration, and the NCS^- content was determined by the method of Volhard. The content of C, N and H in the complex were determined using a Perkin–Elmer 240C Elemental Analyser (U.S.A.). The glycine content was determined with a Hitachi 835 Amino Acid Analyzer (Japan).

Physical measurements

The IR spectra of the complexes were recorded using a Nicolet Model 20SX spectrophotometer. The samples were mounted as mulls in KBr discs and examined between 4000 and 300 cm^{-1}.

The X-ray powder diffractograms of the complexes were obtained with an X-ray diffractometer (D/Hax-rA, Rigaku, Japan) with copper radiation and a nickel filter.

DSC experimental equipment and conditions

DSC experiments on the three complexes were carried out with a Perkin–Elmer DSC-2C differential scanning calorimeter (U.S.A.) and 3600 data station under conditions of an N_2 atmosphere 20 ml min^{-1}) and a heating rate of 5 °C min^{-1}.

The reliability of the temperature system and the calorimetric system was monitored in the present experiments by measuring the melting point and the heat of fusion of indium under an N_2 atmosphere (20 ml min^{-1}) at a heating rate of 5 °C min^{-1}. The measured values were 429.5 K and 3.28 kJ mol^{-1}, which are consistent with the literature values of 429.78 K and 3.27 kJ mol^{-1}.

RESULTS AND DISCUSSION

1. Component analysis of the complexes

The results of component analysis of the complexes are given in Table 1. The formulae weights of all three complexes agree with the general formula $RE(NCS)_3 \cdot 3Gly \cdot H_2O$, where RE = Ce, Pr or Nd.

2. Physical measurements

The IR wavenumbers of some group vibrations in the complexes are listed in Table 2.

If we compare the frequencies of some group vibrations of glycine in free and complexed forms, the results indicate that glycine retains its zwitterionic structure in its rare earth complexes. This excludes the possibility of coordination of nitrogen to the rare earth ions. There thus remains the possibility of attachment of the carboxylic group of glycine to rare earth ions.

The antisymmetric stretch of the carboxylic group of glycine in its complexes shows a shoulder in addition to the main peak. This could be due to more than one kind of bonding of the carboxylate group of the glycine molecule in its rare earth complexes, which may probably be achieved by polymerization of the monomer species. The OH stretch of water molecules in rare earth–glycine complexes has been observed between 3330 and 3370

TABLE 1

Results of component analysis of the complexes

Complex	RE^{3+} (%) C (%)		NCS^- (%) H (%)		Gly (%) N (%)	
	calc.	found	calc.	found	calc.	found
$Ce(NCS)_3 \cdot 3Gly \cdot H_2O$	25.13	25.02	31.25	31.10	40.39	40.36
	19.39	19.35	3.07	3.05	15.08	15.38
$Pr(NCS)_3 \cdot 3Gly \cdot H_2O$	25.24	25.00	31.21	30.87	40.33	39.81
	19.36	19.64	3.07	3.06	15.05	15.23
$Nd(NCS)_3 \cdot 3Gly \cdot H_2O$	25.67	25.81	31.02	31.10	40.10	39.71
	19.24	19.46	3.05	2.99	14.97	14.95

TABLE 2

Wavenumbers (cm^{-1}) of some group vibrations in the complexes [a]

Approximate description of mode	Gly [2]	$Ce(NCS)_3 \cdot 3Gly \cdot H_2O$	$Pr(NCS)_3 \cdot 3Gly \cdot H_2O$	$Nd(NCS)_3 \cdot 3Gly \cdot H_2O$
Vibrations of NH_3^+ group of glycine				
stretch	3170	3090s	3090s	3094s
asymmetric bend	1610	1669s	1662s	1665s
symmetric bend	1520	1492s	1492s	1491s
rock	1104	1105m	1106m	1106m
	1122	1125w	1120w	1124w
Vibrations of COO^- group of glycine				
asymmetric stretch	1587	1567s	1571s	1577s
		1601s	1602s	1602s
symmetric stretch	1407	1410s	1411s	1411s
bend	693	664m	666m	666m
Vibrations of CH_2 group of glycine				
bend	1448	1451s	1452s	1453s
wag	1328	1333s	1333s	1333s
twist	1310	1313w	1311w	1311w
rock	908	905s	904s	905s
Skeletal vibration of glycine				
$C-N^+$ stretch	1024	1040w	1046w	1050w
		1021m	1022m	1023m
C–C stretch	890	770w	768w	772w
Vibrations of OH group of water molecule				
stretch		3333sb	3367sb	3368sb
Vibration of NCS^- group				
stretch of C≡N		2026s	2029s	2029s
		2073s	2072s	2073s

[a] Intensity of peaks: s strong; m medium; w weak; sb strong, broad.

cm^{-1}. This shows that water molecules in the complexes are hydrogen bonded.

Generally speaking, the stretching vibration of C≡N is between 2240 and 2260 cm^{-1}, but in the complexes the stretching has been observed between 2020 and 2075 cm^{-1}. This shows that NCS^- groups in the complexes are coordinated through nitrogen to the rare earth ions.

As an example, the X-ray diffraction data of $Ce(NCS)_3 \cdot 3Gly \cdot H_2O$ and $Ce(NCS)_3 \cdot 7H_2O$ are listed in Table 3. X-ray diffraction data of glycine are also given in Table 3.

From Table 3 we can see that the X-ray diffraction data of $Ce(NCS)_3 \cdot 7H_2O$, $Ce(NCS)_3 \cdot 3Gly \cdot H_2O$ and glycine are different. The prepared complex is not a simple mixture of $Ce(NCS)_3 \cdot 7H_2O$ and glycine.

3. DSC experiments

The DSC curves of the thermal decomposition reactions of the three complexes $RE(NCS)_3 \cdot 3Gly \cdot H_2O$ (RE = Ce, Pr and Nd) are similar. The

TABLE 3

X-Ray diffraction data of $Ce(NCS)_3 \cdot 3Gly \cdot H_2O$, $Ce(NCS)_3 \cdot 7H_2O$ and glycine

Compound	2θ (deg)	I/I_0	2θ (deg)	I/I_0	2θ (deg)	I/I_0	2θ (deg)	I/I_0
$Ce(NCS)_3 \cdot 3Gly \cdot H_2O$	7.62	100	9.52	7.2	10.54	87.0	12.15	11.8
	14.94	20.8	15.51	14.8	20.02	10.8	20.47	26.2
	21.28	18.3	21.80	27.4	23.20	22.4	24.58	29.8
	26.33	6.7	26.95	32.6	27.76	13.2	30.17	5.4
	30.74	15.6	31.56	8.6	32.31	18.3	34.60	7.4
	35.19	14.1	36.16	11.4	37.03	13.7	39.23	9.8
	41.88	10.7	43.76	6.4	44.48	13.4	45.40	9.2
	46.39	7.5	47.16	6.8	47.69	7.1	52.19	8.1
	57.03	5.8	57.61	6.1				
$Ce(NCS)_3 \cdot 7H_2O$	11.70	33.7	13.16	4.3	13.82	100	14.04	33.3
	17.34	68.4	18.24	20.2	20.18	5.3	21.04	44.3
	21.56	29.4	21.70	49.7	24.91	21.3	27.53	4.6
	28.09	5.3	28.65	16.7	28.77	25.9	30.49	6.0
	32.03	8.2	32.85	5.3	33.29	25.8	33.69	8.2
	34.21	14.2	34.49	9.9	35.05	18.4	36.89	56.0
	37.21	27.0	39.43	4.3	39.75	4.3	39.89	3.6
	40.15	21.3	40.83	41.8	41.87	20.6	42.27	7.8
	42.67	3.6	43.23	4.3	43.31	3.6	44.19	8.5
	46.19	6.0	49.31	6.4	50.91	10.6	52.67	3.6
	53.87	3.6	53.99	4.3	55.29	7.1	58.27	9.6
Glycine [2]	8.0	19.0	15.0	37.7	19.1	47.8	20.2	88.9
	24.0	72.6	28.6	31.8	29.4	48.2	30.2	100
	35.4	39.1	36.8	31.1	38.8	28.4	44.4	25.2

DSC curves of the thermal decomposition reactions of $Ce(NCS)_3 \cdot 3Gly \cdot H_2O$ and $Nd(NCS)_3 \cdot 3Gly \cdot H_2O$ are shown in Figs. 1 and 2. The thermal decomposition data of peaks I and II of $RE(NCS)_3 \cdot 3Gly \cdot H_2O$ are summarized in Table 4.

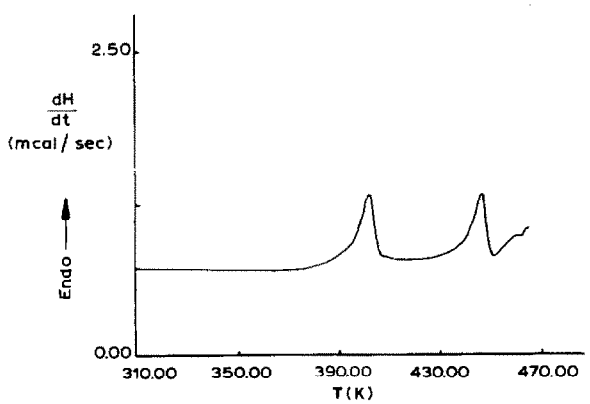

Fig. 1. The DSC curve of $Ce(NCS)_3 \cdot 3Gly \cdot H_2O$ (peak I, peak II).

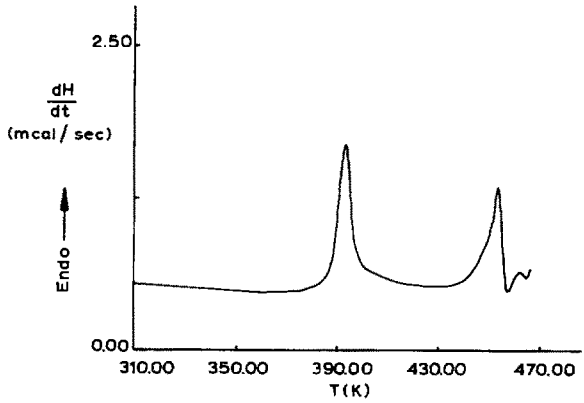

Fig. 2. The DSC curve of $Nd(NCS)_3 \cdot 3Gly \cdot H_2O$ (peak I, peak II).

TABLE 4

Thermal decomposition data of $RE(NCS)_3 \cdot 3Gly \cdot H_2O$ determined by DSC curves (peaks I and II)

	$Ce(NCS)_3 \cdot 3Gly \cdot H_2O$	$Pr(NCS)_3 \cdot 3Gly \cdot H_2O$	$Nd(NCS)_3 \cdot 3Gly \cdot H_2O$
Peak I			
T_{max} (K)	403.29	397.34	393.35
Onset (K)	396.77	394.33	386.90
ΔH(kJ mol^{-1})	39.92	50.11	57.79
T_0 (K)	368.06	377.75	376.32
T_e (K)	414.38	410.00	423.28
Peak II			
T_{max} (K)	447.84	448.37	453.10
Onset (K)	444.20	441.63	447.11
ΔH(kJ mol^{-1})	32.85	32.45	35.72
T_0 (K)	433.50	427.56	432.16
T_e (K)	451.67	454.23	457.09

It can be concluded from Table 4 that the three complexes have similar thermal stabilities and courses of thermal decomposition.

KINETIC EQUATIONS AND ANALYSIS OF KINETIC DATA

In this paper, we use Bagchi and Sen's integral and differential equations [4] to analyze kinetic problems. The integral equation and differential equation are as below

$$\ln\left[\frac{g(\alpha)}{T-T_0}\right] = \ln\left(\frac{A}{\phi}\right) - \frac{E}{RT} \tag{1}$$

$$\ln\left\{\frac{d\alpha/dT}{f(\alpha)\left[E(T-T_0)/RT^2+1\right]}\right\} = \ln\frac{A}{\phi} - \frac{E}{RT} \tag{2}$$

TABLE 5

Several kinetic functions [5] used for the present analysis

Function No.	Function form	
	integral form $g(\alpha)$	differential form $f(\alpha)$
1	$1/2\alpha$	α^2
2	$[-\ln(1-\alpha)]^{-1}$	$\alpha+(1-\alpha)\ln(1-\alpha)$
3	$3[(1-\alpha)^{-1/3}-1]^{-1}/2$	$(1-2\alpha/3)-(1-\alpha)^{2/3}$
4	$3(1-\alpha)^{2/3}[1-(1-\alpha)^{1/3}]^{-1}/2$	$[1-(1-\alpha)^{1/3}]^2$
5	$3(1+\alpha)^{2/3}[(1+\alpha)^{1/3}-1]^{-1}/2$	$[(1+\alpha)^{1/3}-1]^2$
6	$3(1-\alpha)^{4/3}[\{1/(1-\alpha)^{1/3}-1\}]^{-1}/2$	$[1/(1-\alpha)^{1/3}-1]^2$
7	$(1-\alpha)$	$-\ln(1-\alpha)$
8	$3(1-\alpha)[-\ln(1-\alpha)]^{1/3}/2$	$[-\ln(1-\alpha)^{2/3}$
9	$2(1-\alpha)[1-\ln(1-\alpha)]^{1/2}$	$[-\ln(1-\alpha)]^{1/2}$
10	$3(1-\alpha)[-\ln(1-\alpha)]^{2/3}$	$[-\ln(1-\alpha)]^{1/3}$
11	$4(1-\alpha)[-\ln(1-\alpha)]^{3/4}$	$[-\ln(1-\alpha)]^{1/4}$
12	$2(1-\alpha)^{1/2}$	$1-(1-\alpha)^{1/2}$
13	$3(1-\alpha)^{2/3}$	$1-(1-\alpha)^{1/3}$
14	1	α
15	$2\alpha^{1/2}$	$\alpha^{1/2}$
16	$3\alpha^{2/3}$	$\alpha^{1/3}$
17	$4\alpha^{3/4}$	$\alpha^{1/4}$
18	$(1-\alpha)^2$	$(1-\alpha)^{-1}-1$
19	$2(1-\alpha)^{3/2}$	$(1-\alpha)^{-1/2}$

In the above equations, α is the fraction of the reacted material, T is the absolute temperature, $f(\alpha)$ and $g(\alpha)$ are differential and integral mechanism functions respectively, E and A are the derived apparent activation energy and pre-exponential constant, respectively, R is the gas constant, and ϕ is the constant heating rate.

The data are fitted to eqn. (1) by the linear least-squares method on a TI-59 computer.

Equation (2) may be solved by the iterative method on the computer. Any arbitrary value may be assumed for $E(E > 0)$ and, using this value, the value of the expression on the left hand side may be calculated for each data point. When plotted against $1/T$ by the least-squares method, it gives new values of E from the slope and A from the intercept. This modified value of E is used as a starting value for the next iteration, which yields another modified value of E. Thus, after a few iterations, consistent values of E and A can be obtained.

Using the possible forms of $g(\alpha)$ and $f(\alpha)$, from Table 5, the data for $Ce(NCS)_3 \cdot 3Gly \cdot H_2O$ (peak I, Table 6) are analyzed by use of eqns. (1) and (2). The results obtained (Table 7) clearly show that, when all conditions [viz. the values of E and A are in the usual range of the thermal decomposition kinetic parameters for solid complexes (E = 80–250 kJ mol^{-1}, log A =

TABLE 6

Data for $Ce(NCS)_3 \cdot 3Gly \cdot H_2O$ determined by DSC (peak I)

Data point	Ti (K)	α_i	$(dH/dt)_i$ $\times 10^2$ (mJ s^{-1})	$(d\alpha/dT)_i$ $\times 10^2$ (K^{-1})
1	385.99	0.0286	11.63	0.56
2	390.88	0.0792	30.60	1.48
3	394.72	0.1600	56.99	2.76
4	398.22	0.2896	96.52	4.68
5	399.96	0.3902	136.06	6.59
6	401.71	0.5330	191.88	9.30
7	403.46	0.7259	236.06	11.44
8	405.90	0.9349	75.98	3.68
9	407.65	0.9735	21.34	1.03

$T_0 = 368.06$ K, $H_0 = 247.69$ mJ, $\phi - 5\,^{\circ}C\ min^{-1}$.

7–30 s^{-1}, linear correlation coefficient $|r| \approx 1$) and the values of E and A from the two methods are approximately the same] are satisfied at the same time, the probable mechanism function is logically function No. 7, and the general expression is $f(\alpha) = 1 - \alpha$.

TABLE 7

Results of analysis of the thermal decomposition data of $Ce(NCS)_3 \cdot 3Gly \cdot H_2O$ (peak I) by integral [eqn. (1)] and differential [eqn. (2)] methods

Function No.	Integral method			Differential method		
	E(kJ mol^{-1})	ln A (s^{-1})	$-r$	E (kJ mol^{-1})	ln A (s^{-1})	$-r$
1	393.61	110.41	0.9943	283.82	77.14	0.8429
2	407.03	114.10	0.9869			
3	431.66	120.06	0.9974	389.34	107.13	0.9584
4	480.77	135.04	0.9979	452.05	126.27	0.9845
5	362.61	98.61	0.9914	240.34	61.61	0.7867
6	−627.02	−194.37	−0.9344			
7	245.72	67.45	0.9906	251.56	69.11	0.9759
8	148.07	38.26	0.9872			
9	99.25	23.66	0.9822			
10	50.43	9.07	0.9637			
11	26.02	1.77	0.9143			
12	213.03	56.77	0.9742			
13	216.78	57.46	0.9970	192.37	50.03	0.9297
14	173.20	45.14	0.9937	73.67	15.29	0.4189
15	62.99	12.51	0.9915	−ve	−ve	−0.2286
16	26.26	1.63	0.9836			
17	7.90	−1.16	0.9178			
18	362.69	103.38	0.9449			
19	67.17	14.83	0.6226			

TABLE 8

Data for $Pr(NCS)_3 \cdot 3Gly \cdot H_2O$ determined by DSC (peak II)

Data point	T_i (K)	α_i	$(dH/dt)_i$ $\times 10^2$ (mJ s^{-1})	$(d\alpha/dT)_i$ $\times 10^2$ (K^{-1})
1	438.00	0.0532	28.41	1.53
2	440.00	0.0916	43.93	2.37
3	442.00	0.1498	66.69	3.59
4	444.00	0.2380	101.29	5.46
5	445.00	0.2998	128.20	6.91
6	446.00	0.3775	160.50	8.65
7	447.00	0.4742	196.65	10.60
8	448.00	0.5880	222.25	11.97
9	449.00	0.7078	219.66	11.83
10	450.00	0.8223	201.33	10.85

$T_0 = 427.56$ K, $H_0 = 222.74\ \Delta$ mJ, $\phi = 5.00\,^\circ$C min^{-1}.

Similar computational results (see Tables 10 and 11) for the other two complexes, $Pr(NCS)_3 \cdot 3Gly \cdot H_2O$ (original data in Table 8) and $Nd(NCS)_3 \cdot 3Gly \cdot H_2O$ (original data in Table 9), are not illustrated here one by one. The results for the kinetic parameters of the three complexes are listed in Table 12.

THE KINETIC COMPENSATION EFFECT

According to the mathematical expression for the kinetic compensation effect, $\ln A = aE + b$, we fitted the obtained kinetic parameters (E and $\ln A$) from the integral method (see Tables 7, 10 and 11) by the linear

TABLE 9

Data for $Nd(NCS)_3 \cdot 3Gly \cdot H_2O$ determined by DSC (peak II)

Data point	T_i (K)	α_i	$(dH/dt)_i$ $\times 10^2$ (mJ s^{-1})	$(d\alpha/dT)_i$ $\times 10^2$ (K^{-1})
1	441.63	0.0736	34.85	1.96
2	443.73	0.1243	50.38	2.83
3	445.47	0.1848	68.95	3.87
4	447.57	0.2840	96.86	5.44
5	449.67	0.4193	130.16	7.31
6	451.75	0.6057	193.30	10.86
7	452.81	0.7321	230.50	12.95
8	454.91	0.9621	106.52	5.98

$T_0 = 432.16$ K, $H_0 = 130.01$ mJ, $\phi = 5.00\,^\circ$C min^{-1}.

TABLE 10

Results of analysis of the thermal decomposition data of $Pr(NCS)_3 \cdot 3Gly \cdot H_2O$ (peak II) by integral [eqn. (1)] and differential [eqn. (2)] methods

Function No.	Integral method			Differential method		
	E(kJ mol^{-})	ln A (s^{-1})	$-r$	E(kJ mol^{-1})	ln A (s^{-1})	$-r$
1	651.24	168.23	0.9990	592.86	152.47	0.9917
2	702.42	181.54	0.9999	679.01	175.22	0.9984
3	722.47	185.52	0.9999	713.03	182.98	0.9993
4	763.00	196.60	0.9993	778.54	200.81	0.9988
5	596.76	151.09	0.9976	516.52	129.44	0.9843
6	895.86	−ve	0.9938			
7	361.92	91.54	0.9952	419.82	107.14	0.9901
8	207.00	49.99	0.9916	272.34	67.53	0.9832
9	129.52	29.21	0.9850			
10	52.04	8.43	0.9422			
11	13.32	−1.96	0.6293			
12	315.12	78.06	0.9993	324.37	80.55	0.9975
13	330.04	81.73	0.9984	356.02	88.73	0.9967
14	274.17	67.55	0.9993	231.17	55.99	0.9670
15	85.64	17.21	0.9988	70.12	13.07	0.7891
16	22.79	0.43	0.9738			
17	−8.63	−7.96	−0.8028			
18	473.48	122.03	0.9781			
19	−3.24	−5.89	−0.0501			

TABLE 11

Results of analysis of the thermal decomposition data of $Nd(NCS)_3 \cdot 3Gly \cdot H_2O$ (peak II) by integral [eqn. (1)] and differential [eqn. (2)] methods

Function No.	Integral method			Differential method		
	E(kJ mol^{-1})	ln A (s^{-1})	$-r$	E(kJ mol^{-1})	ln A (s^{-1})	$-r$
1	539.31	137.09	0.9973	443.34	111.39	0.9587
2	602.69	153.60	0.9997	562.87	142.93	0.9934
3	630.67	159.68	0.9997	617.94	156.27	0.9982
4	688.89	175.46	0.9978	720.68	183.98	0.9955
5	484.00	119.82	0.9947	366.46	88.39	0.9322
6	898.25	−ve	0.9780			
7	338.43	84.73	0.9849			
8	189.40	45.03	0.9751			
9	114.87	25.17	0.9569			
10	40.36	5.32	0.8224			
11	3.09	−4.61	0.1336			
12	268.85	65.18	0.9985	284.42	69.34	0.9920
13	290.10	70.54	0.9955	333.71	82.15	0.9869
14	215.31	51.35	0.9979	143.21	32.15	0.7829
15	53.32	8.48	0.9988			
16	−0.69	−5.81	−0.1555			
17	−27.68	−12.96	−0.9753			
18	513.85	132.25	0.9411			
19	48.33	8.15	0.3737			

TABLE 12

Calculated values of kinetic parameters of thermal decomposition for the three complexes $RE(NCS)_3 \cdot 3Gly \cdot H_2O$ (RE = Ce, Pr and Nd)

	$Ce(NCS)_3 \cdot 3Gly \cdot H_2O$	$Pr(NCS)_3 \cdot 3Gly \cdot H_2O$	$Nd(NCS)_3 \cdot 3Gly \cdot H_2O$
Peak	I	II	II
α	0.0286–0.9735	0.0532–0.8223	0.0736–0.9621
$g(\alpha)$	$-\ln(1-\alpha)$	$1-(1-\alpha)^{1/2}$	$1-(1-\alpha)^{1/2}$
Integral method			
E (kJ mol^{-1})	245.72	315.12	268.85
ln A (s^{-1})	67.45	78.06	65.18
$-r$	0.9906	0.9993	0.9985
Differential method			
E (kJ mol^{-1})	251.56	324.37	284.42
ln A (s^{-1})	69.11	80.55	69.34
$-r$	0.9757	0.9975	0.9920

least-squares method on a TI-59 computer, and obtained the kinetic compensation parameters a and b. The values of a and b are given in Table 13.

The results in Table 13 show that the differences in the kinetic parameters for a reaction could be determined by both the method of calculation used and the kinetic compensation. The kinetic parameters ln A and E seem to be connected through a and b.

From all the above results, we can see that the mechanisms corresponding to peak II of $Pr(NCS)_3 \cdot 3Gly \cdot H_2O$ and $Nd(NCS)_3 \cdot 3Gly \cdot H_2O$ are the same, and difer from that corresponding to peak I of $Ce(NCS)_3 \cdot 3Gly \cdot H_2O$. On the other hand, the kinetic compensation parameters of $Pr(NCS)_3 \cdot 3Gly \cdot H_2O$ (peak II) and $Nd(NCS)_3 \cdot 3Gly \cdot H_2O$ (peak II) are approximately the same. Therefore we consider that the kinetic compensation parameters may be characteristic of the decomposition reaction itself.

TABLE 13

Calculated values of kinetic compensation parameters of the three complexes

Complex	Peak	a	b	r
$Ce(NCS)_3 \cdot 3Gly \cdot H_2O$	I	0.30	−6.26	0.9998
$Pr(NCS)_3 \cdot 3Gly \cdot H_2O$	II	0.27	−5.28	0.9999
$Nd(NcS)_3 \cdot 3Gly \cdot H_2O$	II	0.26	−5.26	0.9999

REFERENCES

1 B.S. Mathur and T.S. Srivastava, J. Inorg. Nucl. Chem., 32 (1970) 3277.
2 Wu Jigui, Deng Ruwen, Wang Liufang and Yu Ming, Lanzhou Univ., 20(3) (1984) 69.
3 Jing-Zhi Yin, Ben-Gao Jiang, Tong-Shan Sun and Yu-Feng Liu, Thermochim. Acta, 123 (1988) 43.
4 T.P. Bagchi and K.P. Sen, Thermochim. Acta, 51 (1981) 175.
5 Li Yuzeng, Thermal Analysis, Qinghua University Press, Beijing, 1987, p. 94 (in Chinese).